ENERGY DEPENDENCE OF ANTI-KAON-TO-KAON RATIO IN HIGH-ENERGY COLLISIONS — A SIMULATED STUDY

Swarnapratim Bhattacharyya[†]

Department of Physics, New Alipore College
L Block, New Alipore, Kolkata 700053, India

Maria Haiduc, Alina Tania Neagu, Elena Firu

Institute of Space Science, Bucharest, Romania

(Received February 17, 2016; accepted November 8, 2016)

A detailed study of energy dependence of $\frac{K^-}{K^+}$ ratio has been carried out in nucleus–nucleus (AA) collisions (Pb+Pb collisions at $\sqrt{s_{NN}} = 6.3$ GeV and 17.3 GeV, Au+Au collisions at $\sqrt{s_{NN}} = 19.6$–200 GeV) and in pp collisions at $\sqrt{s} = 6.3$–200 GeV in the framework of UrQMD and DPMJET III models. It has been observed that as energy increases, the $\frac{K^-}{K^+}$ ratio increases systematically for both nucleus–nucleus and pp collisions. A comparison of our analysis with the analysis of the experimental data has also been presented wherever available. Our analysis is well-supported by the experimental results obtained by different collaborations in different times.

DOI:10.5506/APhysPolB.47.2347

1. Introduction

Heavy-ion collisions at relativistic and ultra-relativistic energy can be used to study the nuclear matter at high temperature and density. Particle production at all the incident energies is a key quantity to extract information on the properties of nuclear matter under these extreme conditions. However, it may be mentioned here that multiparticle production in high-energy collisions is still a mystery, as far as the understanding of the dynamics of the production of secondaries, especially of the soft varieties, is concerned. Of the various types of particles produced, mesons, especially the π-mesons, constitute, in practical terms, the near totality of the produced particles. In high-energy collisions along with pions, kaons are also produced.

[†] Corresponding author: swarna_pratim@yahoo.com

Kaons are important due to their strangeness content and because they are supposedly related with the physics of the postulated quark–gluon plasma (QGP) signatures [1]. It has been suggested that strangeness production is a sensitive probe of a deconfined state: for example, strangeness production may be enhanced by the fast and energetically favourable process of gluon–gluon fusion into strange quark–anti-quark pairs [2]. Hadronic mechanisms, on the other hand, may also enhance the strangeness production. A systematic investigation of strangeness production may, therefore, provide a crucial input for understanding the matter created in heavy-ion collisions. It should be mentioned here that kaons are the lightest from the variety of the measurable strange particles and kaon production is considered to have a bearing on the nuclear equation of state as indicated by Sturm *et al.* [3].

Microscopic transport calculations indicate that the yield of kaons created in collisions between heavy nuclei at sub-threshold beam energies is sensitive to the compressibility of nuclear matter at high baryon densities [4, 5]. This sensitivity is due to the production mechanism of positive K mesons (K^+). At sub-threshold beam energies, the production of kaons requires multiple nucleon–nucleon collisions or secondary collisions. These processes are expected to occur predominantly at high baryon densities, and the densities reached in the fireball depend on the nuclear equation of state [6]. Positive kaons are well-suited to probe the properties of the dense nuclear medium because of their long mean free path. The propagation of K^+ mesons in nuclear matter is characterized by the absence of absorption (as they contain an anti-strange quark) and, hence, kaons emerge as messengers from the dense phase of the collision. The influence of the medium on the K^+ yield is amplified by the steep excitation function of kaon production near threshold energies. Early transport calculations find that the K^+ yield from Au+Au collisions at sub-threshold energies will be enhanced by a factor of about two if a soft rather than a hard equation of state is assumed [4, 5].

The yields of negative kaons (K^-) and positive kaons (K^+) together provide a sensitive probe of the space-time evolution of heavy-ion reactions. Since the negative kaons (K^-) have a large annihilation cross section with neutrons, their yield is sensitive to the baryon density. The K^- and K^+ distributions may also hint at the degree of thermalization achieved, and their transverse mass spectra allow a detailed study of rescattering and collective expansion effects. Different studies of kaon production take into account the modification of the kaon properties in the dense nuclear medium [7, 8]. When assuming a repulsive K^+N potential as proposed by various theoretical models [9], the energy needed to create a K^+ meson in the nuclear medium is increased and, consequently, the K^+ yield will be reduced. Therefore, the yield of K^+ mesons produced in heavy-ion collisions is affected by both the nuclear compressibility and the in-medium kaon potential.

The anti-particle-to-particle ratio in high-energy interactions is important indicator of the collision dynamics. By comparing large and small systems over a wide range of phase space, one can address both reaction mechanisms in simpler systems and the properties of hot and dense nuclear matter in large systems. Along with the study of heavy-ion collisions, a thorough understanding of proton–proton (pp) collisions at ultra-relativistic energies is also necessary both as input to detailed theoretical models of strong interactions, and as a baseline for understanding the more complex nucleus–nucleus collisions at the RHIC energies. Soft particle production from ultra-relativistic pp collisions is also sensitive to the flavour distribution within the proton, quark hadronization and baryon number transport.

In this paper, we are presenting an analysis of energy dependence of anti-kaon-to-kaon ratio in nucleus–nucleus (AA) collisions (Pb+Pb collisions at $\sqrt{s_{NN}}$ = 6.3 GeV and 17.3 GeV, Au+Au collisions at $\sqrt{s_{NN}}$ = 19.6–200 GeV) and in pp collisions at $\sqrt{s}$ = 6.3–200 GeV in the framework of UrQMD and DPMJET III models. We have also compared our results with available experimental results obtained so far. Before going into the details of the analysis, it will be convenient for the readers to have brief introduction about the two models.

2. UrQMD and DPMJET III models — a brief introduction

2.1. UrQMD model

UrQMD model is a microscopic transport theory, based on the covariant propagation of all the hadrons on the classical trajectories in combination with stochastic binary scattering, colour string formation and resonance decay. It represents a Monte Carlo solution of a large set of coupled partial integro-differential equations for the time evolution of various phase space densities. The basic input to this transport model is that a hadron–hadron interaction would occur if the relative distance (d_{trans}) between the two particles in three-dimensional configuration space satisfies the relation $d_{\text{trans}} \leq d_0 = \sqrt{\frac{\sigma_{\text{tot}}}{\pi}}$ [10–12]. The total cross section σ_{tot} depends on the centre-of-mass energy, the species and the quantum number of the incoming particles. At the point of closest approach, this distance is purely transverse with regard to the relative velocity vector of the particles. In UrQMD model, the Fermi gas model has been utilized to describe the projectile and the target nuclei, the initial momentum of each nucleon being distributed at random between zero and the local Thomas–Fermi momentum. Each nucleon is described by a Gaussian-shaped density distribution, and the wave function for each nucleus is taken as a product of single nucleon Gaussian functions without taking into account the Slater determinant necessary for anti-symmetrization. In the configuration space, the centroids of the

Gaussian functions are distributed at random within a sphere, and finite widths of these Gaussian functions result in a diffused surface region. At low and intermediate energies, typically $\sqrt{s} < 5$ GeV, the phenomenology of hadronic physics has been described in terms of interactions between known hadrons and their resonances. At energies above 5 GeV, the excitation of colour strings and their subsequent fragmentation into hadrons dominate the particle production mechanism. The rescattering effects are also nicely implemented into the model. The UrQMD collision term contains 55 different baryon species (including nucleon, delta and hyperon resonances with masses up to 2.25 GeV/c^2) and 32 different meson species (including strange meson resonances), which are supplemented by their corresponding anti-particle and all isospin-projected states. The states can either be produced in string decays, s-channel collisions or resonance decays. This model can be used in the entire available range of energies from the Bevalac region to RHIC. For more details about this model, readers are requested to consult [10–12].

2.2. DPMJET III model

The Monte Carlo event generator DPMJET can be used to study particle production in high-energy nuclear collisions including photo-production and deep inelastic scattering off the nuclei. It is a code system based on the Dual Parton Model and unifies all features of the DTUNUC-2, DPMJET II and PHOJET1.12 event generators. DPMJET III allows the simulation of hadron–hadron, hadron–nucleus, nucleus–nucleus, photon–hadron, photon–photon and photon–nucleus interactions from a few GeV up to the highest cosmic ray energies. DPMJET is an implementation of the two-component Dual Parton Model for the description of interactions involving nuclei. This model is based on the Gribov–Glauber [13–15] approach. Gribov theory of high-energy interactions of hadrons and nuclei is based on general properties of amplitudes in relativistic quantum theory and provides a unified approach to a broad class of processes. According to this theory, the Glauber approximation [15] to nuclear dynamics is valid in the region of not too high energies and should be modified at energies of RHIC and LHC. Gribov theory then allows to determine the corrections to the Glauber approximation [15] for inclusive particle spectra by relating them to cross sections of large-mass diffraction. The technique has been applied to calculation of shadowing effects for structure functions of nuclei and a good agreement with experimental data on these processes has been obtained. The same approach predicts a strong reduction of particle densities at super-high energies as compared to predictions of the Glauber approximation [15]. Since its first implementations [16], DPMJET model uses the Monte Carlo realization of the Gribov–Glauber multiple scattering formalism according to the algorithms of [17] and allows the calculation of total, elastic, quasi-

elastic and production cross sections for any high-energy nuclear collision. DPMJET III model treats both soft and hard scattering processes in a unified way. Soft processes are parametrized according to Regge phenomenology, whereas lowest order perturbative QCD is used to simulate the hard component. In this model, the multiple parton interactions in each individual hadron/nucleon/photon–nucleon interaction are described by the PHOJET event generator and the fragmentation of parton configurations is treated by the Lund model PYTHIA. For a detailed discussion about the model, one may consult [18, 19].

2.3. Difference between UrQMD and DPMJET III models

In order to present the physical difference between UrQMD and DPMJET III models we should remember that a classification of models for heavy-ion collisions is always delicate due to the fact that most of them are mixed models. They contain different physical assumptions for each stage of the collision. It may be mentioned here that both UrQMD and DPMJET III are microscopic Monte Carlo models. UrQMD is a hadronic transport model and DPMJET III is based on string interaction. String models describe the collision through the exchange of colour or momentum between partons in the projectile and target. As a consequence of these exchanges, these partons become joined by colourless objects which are called string, ropes or flux tubes. These models were originally designed for hadron–hadron, its generalization to hadron–nucleus and nucleus–nucleus were done through the Glauber–Gribov theory [13–15]. pQCD computed parton–parton collisions are included in these models so that they contain a soft and a hard component which is crucial for their application to RHIC and LHC energies.

In hadronic transport models, on the other hand, a relativistic Boltzmann equation is solved for hadrons in the final stage of the collision (after hadronization). Examples of hadronic transport models are AMPT [20–22], RQMD [23–26], UrQMD [10–12] and HSD [27, 28]. UrQMD is a semi-classical hadronic transport model based on the concepts of kinetic theory, in which the evolution of a heavy-ion collision is described by the propagation of on-shell particles on relativistic trajectories in combination with a stochastic treatment of the individual particle scattering processes. The model offers an effective solution for the relativistic Boltzmann equation, where the collision term includes elastic and inelastic scatterings as well as resonance decays. To account for the quantum statistics, the hadrons are represented by Gaussian wave packets and effects such as, *e.g.*, Pauli blocking are included in this model. Both UrQMD [29–35] and DPMJET III [36–38] models have been applied successfully to study high-energy collisions.

3. Analysis and results

We have generated a large sample of events using the UrQMD (UrQMD-3.3p1) [10–12] and DPMJET III (DPMJET 3.06) [18, 19] models in Pb+Pb collisions at $\sqrt{s_{NN}}$ = 6.3 GeV and 17.3 GeV, and in Au+Au collisions at $\sqrt{s_{NN}}$ = 19.6 GeV, 62.4 GeV and 200 GeV. We have calculated the number of positive and negative kaons from the generated output of the UrQMD and DPMJET III models. The ratios of negative-to-positive kaon $\frac{K^-}{K^+}$ at these different collision energies for two different nucleus–nucleus interactions have been evaluated and presented in Table I for both UrQMD and DPMJET III simulated events. It can be noticed from the table that as energy increases, the $\frac{K^-}{K^+}$ ratio increases systematically for both UrQMD and DPMJET III models. From the table, it can be noted that in the case of Pb+Pb collisions at $\sqrt{s_{NN}}$ = 6.3 GeV, the $\frac{K^-}{K^+}$ ratio for UrQMD and DPMJET III are almost the same. But at $\sqrt{s_{NN}}$ = 17.3 GeV, a considerable difference between the UrQMD and DPMJET III simulated results occurs. At higher energy, the DPMJET III simulated values of $\frac{K^-}{K^+}$ in the case of Au+Au collisions overestimate the UrQMD simulated values significantly.

TABLE I

The values of $\frac{K^-}{K^+}$ in nucleus–nucleus (AA) collisions (Pb+Pb collisions at $\sqrt{s_{NN}}$ = 6.3 GeV and 17.3 GeV, Au+Au collisions at $\sqrt{s_{NN}}$ = 19.6–200 GeV) in the framework of UrQMD and DPMJET III models simulation performed by us and also the experimental values published at different times.

Interactions	Energy $\sqrt{s_{NN}}$ [GeV]	UrQMD simulated values of our analysis	DPMJET III simulated values of our analysis	Experimentally obtained values	Reference for experimental data
		$\frac{K^-}{K^+}$	$\frac{K^-}{K^+}$	$\frac{K^-}{K^+}$	
Pb+Pb collisions	6.3	.300	.297	.253 ± .010	[39]
	17.3	.585	.655	.503 ± .012	[40]
Au+Au collisions	19.6	.609	.772	.600 ± .002	[41]
	62.4	.757	.897	.850 ± .004	[42]
	200	.847	.947	.933 ± .007	[43]

The experimental studies of the anti-kaon-to-kaon ratio at different energies in nucleus–nucleus (AA) collisions have been carried out by different collaborations. From their published papers, we have extracted the values of $\frac{K^-}{K^+}$ ratio and tabulated the values in Table I for AA collisions along with the UrQMD and DPMJET III models simulated values. The experimental values of $\frac{K^-}{K^+}$ ratio in Pb+Pb collisions have been calculated from [39] for $\sqrt{s_{NN}}$ = 6.3 GeV and from [40] for $\sqrt{s_{NN}}$ = 17.3 GeV. In the case

of Au+Au collisions, the experimental values of $\frac{K^-}{K^+}$ ratio have been calculated from [41] at $\sqrt{s_{NN}} = 19.6$ GeV, from [42] for $\sqrt{s_{NN}} = 62.4$ GeV and from [43] at $\sqrt{s_{NN}} = 200$ GeV. From Table I, it is reflected that the calculated ratio of anti-kaon-to-kaon as obtained from the experimental analysis in AA collision is found to be lower than the UrQMD and DPMJET III models calculated values at $\sqrt{s_{NN}} = 6.3$, 17.3 and 19.6 GeV. At higher energies however, the experimentally calculated $\frac{K^-}{K^+}$ ratio for AA collision has been found to be higher than UrQMD simulated values but lower than the DPMJET III simulated values.

From Table I, it is also seen that the experimentally obtained $\frac{K^-}{K^+}$ values increase with the increase of energy. It has been pointed out in [40] that the $\frac{K^-}{K^+}$ ratio increases with the energy from about 0.15 at low AGS energy [44–50] to about 0.5 at SPS energy [51, 52] and reaches about 0.9 at RHIC energy [40]. The explanation of the energy dependence of $\frac{K^-}{K^+}$ values can be obtained from the underlying physics of kaon and anti-kaon production mechanism. There are two possible mechanisms of kaon production. Pair production of kaon and anti-kaon is one of them. Another mechanism is the associated production mechanism. The associated production mechanism can only produce K^+ mesons via the following two interactions: $N + N \rightarrow N + X + K^+$ and $\pi + N \rightarrow X + K^+$, where N is the nucleon and X is either Λ hyperons or Ξ hyperons. The pair production mechanism produces K^+ and K^- according to the interaction given by $N + N \rightarrow N + N + K^+ + K^-$. The rise of $\frac{K^-}{K^+}$ ratio as a function of energy can be attributed to the nature of kaon production channels. At the lower energy, the associated production dominates. As the energy increases, the pair production which produces the same number of K^+ and K^- becomes more significant. At higher energy, the anti-kaon excitation function is steeper than that of the kaon because of a higher threshold. So at higher energy, the anti-kaon production cross section increases faster than that of kaon and the ratio increases.

It has been pointed out in [53] that the $\frac{K^-}{K^+}$ ratio can be interpreted as an indirect measure of the baryon chemical potential. If the central region in a nucleus–nucleus collision were net baryon-free ($\mu_B = 0$), then the $\frac{K^-}{K^+}$ ratio would be equal to one, and according to both coalescence model [42, 54] and statistical model [43], the anti-baryon-to-baryon ratios would also be equal to one, under the assumption that strangeness is locally conserved.

In order to compare the values of $\frac{K^-}{K^+}$ obtained from heavy-ion collisions to those from hadron–hadron collisions, we have also simulated the proton–proton collision data at $\sqrt{s} = 6.3$, 17.3, 19.6, 62.4 and 200 GeV using both UrQMD model and the DPMJET III model. We have calculated the values of $\frac{K^-}{K^+}$ from the output of these two models for pp collisions at these above mentioned energies. The values of $\frac{K^-}{K^+}$ at $\sqrt{s} = 6.3$–200 GeV in the case

of *pp* collisions have been tabulated in Table II. From the table, it can be noticed that for *pp* collisions also the ratio of $\frac{K^-}{K^+}$ increases systematically with energies for both UrQMD and DPMJET III models. In the case of *pp* collisions however, at lower energy regime ($\sqrt{s}$ = 6.3, 17.3 and 19.6 GeV), the $\frac{K^-}{K^+}$ ratios calculated from DPMJET III simulation are found to be slightly lower than their UrQMD counterparts. On the other hand, at $\sqrt{s}$ = 62.4 GeV and 200 GeV, DPMJET III simulated values are a little higher than the UrQMD simulated values. Thus, from Tables I and II, it may be said that the UrQMD and DPMJET III give almost the same value for *pp* collisions but the values for nucleus–nucleus collisions differ. This is an interesting observation. A heavy-ion system has multiple initial collisions as well as significant re-scattering and may reach thermal equilibrium before freeze out occurs, while the significantly smaller *pp* system should not interact much beyond the initial reactions. This is reflected in the behaviour of the two models.

TABLE II

The values of $\frac{K^-}{K^+}$ in *pp* collisions at $\sqrt{s}$ = 6.3–200 GeV in the framework of UrQMD and DPMJET III models along with the experimentally obtained values.

Interactions	Energy $\sqrt{s_{NN}}$ [GeV]	UrQMD simulated values of our analysis	DPMJET III simulated values of our analysis	Experimentally obtained values	Reference for experimental data
		$\frac{K^-}{K^+}$	$\frac{K^-}{K^+}$	$\frac{K^-}{K^+}$	
	6.3	.303	.289	$.247 \pm .007$	[55]
	17.3	.638	.637	$.575 \pm .009$	[56]
pp	19.6	.690	.649	not available	not available
collisions	62.4	.807	.813	$.922 \pm .027 \pm .046$	[57]
				$.97 \pm .05(\text{stat}) \pm .07(\text{syst})$	[58]
	200	.875	.889	$.94 \pm .08$	[59]
				$.93 \pm .05(\text{stat}) \pm .03(\text{syst})$	[60]

The main ingredients of the UrQMD model are the cross sections of binary reactions, the two-body potentials and decay widths of resonances. Strange hadron production in the UrQMD model proceeds through different channels — the excitation and de-excitation (decay) of hadronic resonances, the excitation and de-excitation of a string and the annihilation of a particle with its anti-particle. The probabilities of different processes are governed by their reaction cross sections. The cross sections serve as an input for the model and are, wherever possible, taken from the experimental measure-

ments of elementary (binary) collisions. Hadronic transport model UrQMD can thus provide a reasonable description of the observed particle ratio and, therefore, can also be described as producing hadrons in apparent equilibrium. However the advantage of the dynamic microscopic model is that one can investigate in detail the particle production and find out at which point during the interaction of the equilibrium it takes place and how long the system remains in such a state.

The main ingredients of DPMJET III model are the string junction transport and the percolation of string as a collective mechanism. The variation of anti-kaon-to-kaon ratio with energy when explained by DPMJET III model is the effect of percolation and string junction also due to the re-scattering that the DPMJET III has switched on.

Experimentally calculated values of $\frac{K^-}{K^+}$ at $\sqrt{s} = 6.3$–200 GeV in the case of *pp* collisions have been tabulated in Table II. Table II reflects that the experimentally calculated $\frac{K^-}{K^+}$ values in *pp* collisions at $\sqrt{s} = 6.3$ GeV [55] and at $\sqrt{s} = 17.3$ GeV [56] are found to be lower than UrQMD and DPMJET III calculated values at the corresponding energy. A study of anti-kaon-to-kaon ratio in *pp* collisions at $\sqrt{s} = 62.4$ GeV has been carried out by the PHENIX

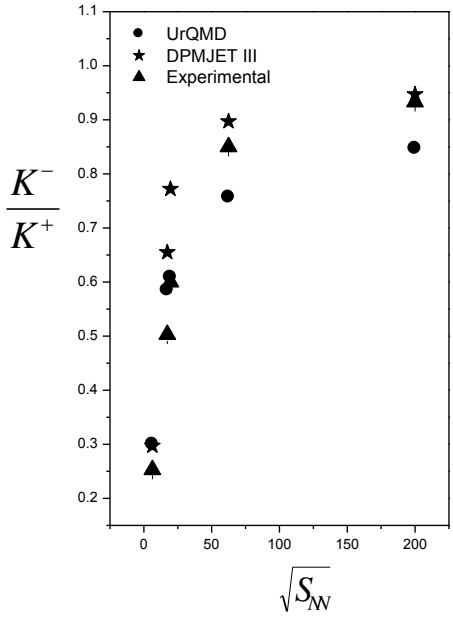

Fig. 1. Variation of the ratio of negative-to-positive kaon $\frac{K^-}{K^+}$ with energy $\sqrt{s_{NN}}$ in nucleus–nucleus collisions (Pb+Pb collisions at $\sqrt{s_{NN}} = 6.3$ GeV and 17.3 GeV, Au+Au collisions at $\sqrt{s_{NN}} = 19.6$–200 GeV) in the framework of UrQMD, DPMJET III models and experimental data.

Collaboration [57]. At $\sqrt{s} = 200$ GeV, the BRAHMS Collaboration [58], STAR Collaboration [59] and PHOBOS Collaboration [60] studied the anti-kaon-to-kaon ratio in proton–proton collisions. In the case of *pp* collisions at $\sqrt{s} = 62.4$ GeV and $\sqrt{s} = 200$ GeV, experimental values of $\frac{K^-}{K^+}$ are found to be higher than the values calculated by UrQMD and DPMJET III simulations as evident from Table II. In the case of *pp* collisions, it is also seen that the experimentally obtained $\frac{K^-}{K^+}$ ratio increases with the increase of energy. We have plotted the variation of $\frac{K^-}{K^+}$ ratio with energy of collisions in figure 1 for nucleus–nucleus and in figure 2 for *pp* collisions for the UrQMD, DPMJET III and the experimental analysis.

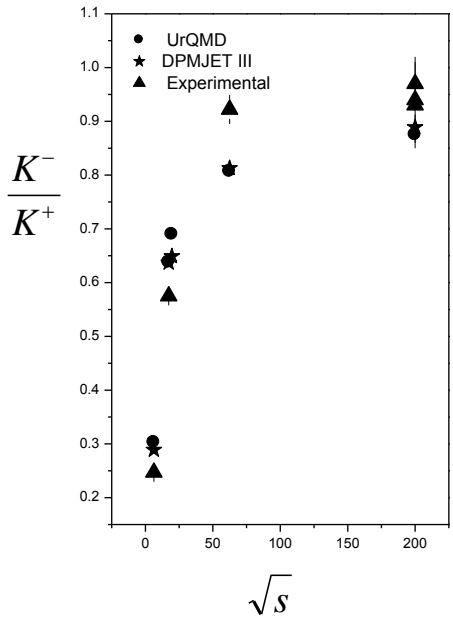

Fig. 2. Variation of the ratio of negative-to-positive kaon $\frac{K^-}{K^+}$ with energy $\sqrt{s}$ in *pp* collisions at $\sqrt{s} = 6.3$–200 GeV for the UrQMD, DPMJET III analysis performed by us and also for the experimental data extracted from the papers of different collaborations.

4. Summary

Let us summarize our findings:

1. The present study of the nature of energy dependence $\frac{K^-}{K^+}$ ratio in the light of UrQMD and DPMJET III simulation agree well with the nature of energy dependence $\frac{K^-}{K^+}$ ratio obtained from the previous experimental observations for both nucleus–nucleus and *pp* collisions.

2. The $\frac{K^-}{K^+}$ ratio increases almost three times from 6.3 GeV to 200 GeV for both nucleus–nucleus and *pp* collisions for UrQMD and DPMJET III simulations. Previous studies of experimental analysis also support this observation for both nucleus–nucleus and *pp* collisions.

3. The energy dependence of $\frac{K^-}{K^+}$ ratio can be attributed to the production mechanism of kaon and anti-kaon.

This work was supported by the grant of the Romanian National Authority for Scientific Research, UEFISCDI, project number PN-II-ID-PCE-2011-3-0978, Contract No. 69/05.10.2011. S. Bhattacharyya acknowledges Prof. Nestor Armesto of Universidade de Santiago de Compostela, Spain for helping in using the DPMJET III code, Prof. F.W. Bopp, Department of Physics, University of Seigen for useful discussions on the difference between UrQMD and DPMJET III models, Prof. Dipak Ghosh, Department of Physics, Jadavpur University and Prof. Argha Deb Department of Physics, Jadavpur University for their inspiration in the preparation of this manuscript.

REFERENCES

[1] J.I. Kapusta, *J. Phys. G* **27**, 593 (2001).
[2] C. Adler *et al.*, *Phys. Lett. B* **595**, 143 (2004) and references therein.
[3] C. Sturm *et al.*, *Phys. Rev. Lett.* **86**, 39 (2001).
[4] J. Aichelin, C.M. Ko, *Phys. Rev. Lett.* **55**, 2661 (1985).
[5] G.Q. Li, C.M. Ko, *Phys. Lett. B* **349**, 405 (1995).
[6] C. Fuchs *et al.*, *Phys. Rev. C* **56**, R606 (1997).
[7] C.M. Ko, G.Q. Li, *J. Phys. G* **22**, 1673 (1996).
[8] W. Cassing, E. Bratkovskaya, *Phys. Rep.* **308**, 65 (1999).
[9] J. Schaffner-Bielich, J. Bondorf, I.N. Mishustin, *Nucl. Phys. A* **625**, 325 (1997).
[10] M. Bleicher *et al.*, *J. Phys. G* **25**, 1859 (1999).
[11] S.A. Bass *et al.*, *Prog. Part. Nucl. Phys.* **41**, 255 (1998).
[12] H. Petersen, M. Bleicher, S.A. Bass, H. Stöcker, `arXiv:0805.0567v1 [hep-ph]` (May 5, 2008).
[13] V.N. Gribov, *Sov. Phys. JETP* **29**, 483 (1969) [*Zh. Eksp. Teor. Fiz.* **56**, 892 (1969)].
[14] N. Armesto *et al.*, *Eur. Phys. J. C* **68**, 447 (2010).
[15] R.J. Glauber, *Lectures on Theoretical Physics*, Vol. 1, W.E. Britten and L.G. Duham Eds., New York, Inter Science, 1959, p. 315.

[16] J. Ranft, *Phys. Rev. D* **51**, 64 (1995).
[17] S.Y. Shmakov, V.V. Uzhinskii, A.M. Zadoroshny, *Comput. Phys. Commun.* **54**, 125 (1989).
[18] S. Roesler, R. Engel, J. Ranft, `arXiv:hep-ph/0012252v1` (December 18, 2000).
[19] F.W. Bopp *et al.*, *Phys. Rev. C* **77**, 014904 (2008).
[20] Z.W. Lin *et al.*, *Phys. Rev. C* **72**, 064901 (2005).
[21] Z.W. Lin *et al.*, *Phys. Rev. C* **64**, 011902 (2001).
[22] B. Zhang *et al.*, *Phys. Rev. C* **61**, 067901 (2000).
[23] H. Sorge, *Phys. Rev. C* **52**, 3291 (1995).
[24] H. Sorge, *Z. Phys. C* **67**, 479 (1995).
[25] M. Berenguer, H. Sorge, W. Greiner, *Phys. Lett. B* **332**, 15 (1994).
[26] H. Sorge *et al.*, *Nucl. Phys. A* **498**, 567c (1989).
[27] J. Geiss *et al.*, *Nucl. Phys. A* **644**, 107 (1998).
[28] W. Cassing, E.L. Bratkovskaya, S. Juchem, *Nucl. Phys. A* **674**, 249 (2000).
[29] J. Steinheimer, M. Bleicher, *EPJ Web Conf.* **97**, 00026 (2015).
[30] Iu.A. Karpenko, P. Huovinen, H. Petersen, M. Bleicher, *Phys. Rev. C* **91**, 064901 (2015).
[31] K.C. Liu, J. Song, F.L. Shao, *Int. J. Mod. Phys. E* **23**, 1450060 (2014).
[32] V.Yu. Vovchenko, D.V. Anchishkin, M.I. Gorenstein, *Phys. Rev. C* **90**, 024916 (2014).
[33] V.V. Begun *et al.*, *J. Phys. G* **42**, 075101 (2015).
[34] D. Ghosh, A. Deb, S. Bhattacharyya, U. Datta, *J. Phys. G* **39**, 105101 (2012).
[35] S. Bhattacharyya, M. Haiduc, A.T. Neagu, E. Firu, *J. Phys. G* **41**, 075106 (2014).
[36] F.W. Bopp *et al.*, *Acta Phys. Pol. B* **35**, 303 (2004).
[37] J. Ranft *et al.*, *Nucl. Phys. Proc. Suppl.* **122**, 392 (2003).
[38] A. Ibarra, S. Wild, *Phys. Rev. D* **88**, 023014 (2013).
[39] C. Alt *et al.*, *Phys. Rev. C* **77**, 024903 (2008).
[40] S.V. Afanasiev *et al.* [NA49 Collaboration], *Phys. Rev. C* **66**, 054902 (2002).
[41] D. Cebra [STAR Collaboration], `arXiv:0903.4702v1 [nucl-ex]` (March 26, 2009).
[42] I.C. Arsene *et al.* [BRAHMS Collaboration], *Phys. Lett. B* **687**, 36 (2010) [`arXiv:0911.2586v2 [nucl-ex]`] (March 12, 2010).
[43] S.S. Adler *et al.*, *Phys. Rev. C* **69**, 034909 (2004).
[44] L. Ahle *et al.* [E802 Collaboration], *Phys. Rev. C* **57**, 466 (1998).
[45] L. Ahle *et al.* [E802 Collaboration], *Phys. Rev. C* **58**, 3523 (1998).
[46] L. Ahle *et al.* [E802 Collaboration], *Phys. Rev. C* **60**, 044904 (1999).

[47] L. Ahle *et al.* [E866 and E917 collaborations], *Phys. Lett. B* **476**, 1 (2000).
[48] L. Ahle *et al.* [E866 and E917 collaborations], *Phys. Lett. B* **490**, 53 (2000).
[49] J. Barrette *et al.* [E877 Collaboration], *Phys. Rev. C* **62**, 024901 (2000).
[50] D. Pelte *et al.* [FOPI Collaboration], *Z. Phys. A* **357**, 215 (1997).
[51] K. Adcox *et al.* [PHENIX Collaboration], *Phys. Rev. Lett.* **88**, 242301 (2002).
[52] B.B. Back *et al.* [PHOBOS Collaboration], *Phys. Rev. Lett.* **87**, 102301 (2001).
[53] J. Adams *et al.* [STAR Collaboration], *Phys. Lett. B* **567**, 167 (2003).
[54] A. Bialas, *Phys. Lett. B* **442**, 449 (1998).
[55] A. Aduszkiewicz *et al.* [NA61 Collaboration], Report CERN-SPSC-2015-036/SPSC-SR-171 (October 14, 2015).
[56] T. Anticic *et al.* [NA49 Collaboration], *Eur. Phys. J. C* **68**, 1 (2010).
[57] A. Adare *et al.* [PHENIX Collaboration], *Phys. Rev. C* **83**, 064903 (2011).
[58] I.G. Bearden *et al.* [BRAHMS Collaboration], *Phys. Lett. B* **607**, 42 (2005).
[59] B.I. Abelev *et al.* [STAR Collaboration], *Phys. Rev. C* **75**, 064901 (2007).
[60] B.B. Back *et al.* [PHOBOS Collaboration], *Phys. Rev. C* **71**, 021901 (2005).